Article

Cancer Cell

Kinase and BET Inhibitors Together Clamp Inhibition of PI3K Signaling and Overcome Resistance to Therapy

Graphical Abstract

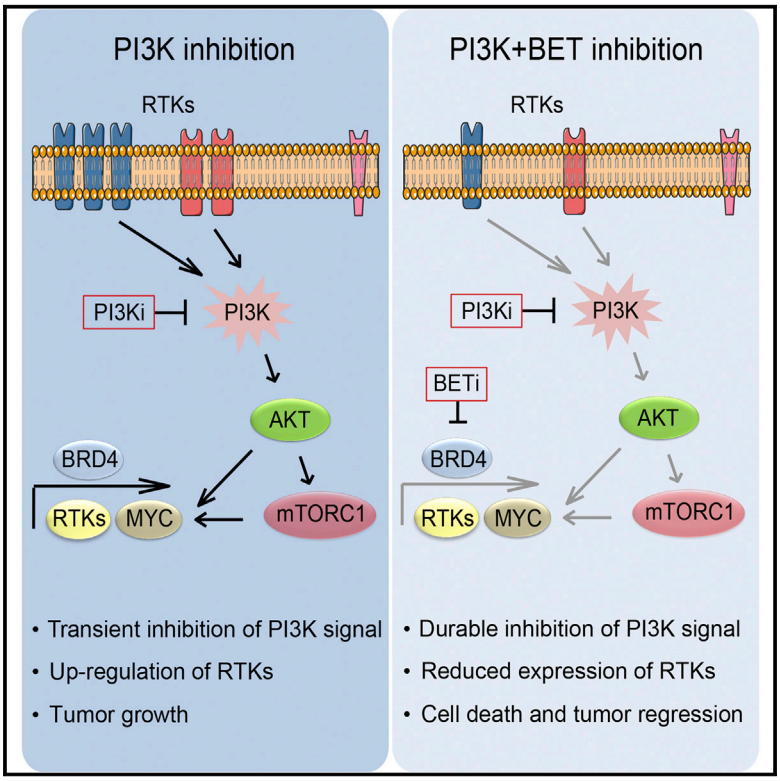

Highlights

- BET inhibitors lower the expression of RTKs and the PI3K signal
- BET inhibition blocks BRD4 binding at the promoter of several RTKs
- Activation of AKT, mTOR, and MYC due to PI3K inhibition is blocked by BET inhibitors
- Targeting BRD4 and PI3K together, but not alone, inhibits growth of many tumor cells

Authors

Elias E. Stratikopoulos, Meaghan Dendy, ..., Ming-Ming Zhou, Ramon Parsons

Correspondence

ramon.parsons@mssm.edu

In Brief

Inhibition of PI3K induces feedback activation of upstream RTKs and quick rebound of the pathway activity. Stratikopoulos et al. show that BRD4 is important for the feedback activation of many RTKs and that combined PI3K and BET inhibition sustains PI3K pathway inhibition and enhances tumor cell killing.

Stratikopoulos et al., 2015, Cancer Cell *27*, 837–851
June 8, 2015
http://dx.doi.org/10.1016/j.ccell.2015.05.006

CellPress

Cancer Cell
Article

Kinase and BET Inhibitors Together Clamp Inhibition of PI3K Signaling and Overcome Resistance to Therapy

Elias E. Stratikopoulos,[1] Meaghan Dendy,[1] Matthias Szabolcs,[2] Alan J. Khaykin,[1] Celine Lefebvre,[3] Ming-Ming Zhou,[4] and Ramon Parsons[1,*]
[1]Department of Oncological Sciences, Icahn School of Medicine at Mount Sinai, 1470 Madison Avenue, New York, NY 10029, USA
[2]Department of Pathology, Columbia University Medical Center, New York, NY 10032, USA
[3]Inserm U981, Institut Gustave Roussy, 94805 Villejuif, France
[4]Department of Structural and Chemical Biology, Icahn School of Medicine at Mount Sinai, 1470 Madison Avenue, New York, NY 10029, USA
*Correspondence: ramon.parsons@mssm.edu
http://dx.doi.org/10.1016/j.ccell.2015.05.006

SUMMARY

Unsustained enzyme inhibition is a barrier to targeted therapy for cancer. Here, resistance to a class I PI3K inhibitor in a model of metastatic breast cancer driven by PI3K and MYC was associated with feedback activation of tyrosine kinase receptors (RTKs), AKT, mTOR, and MYC. Inhibitors of bromodomain and extra terminal domain (BET) proteins also failed to affect tumor growth. Interestingly, BET inhibitors lowered PI3K signaling and dissociated BRD4 from chromatin at regulatory regions of insulin receptor and EGFR family RTKs to reduce their expression. Combined PI3K and BET inhibition induced cell death, tumor regression, and clamped inhibition of PI3K signaling in a broad range of tumor cell lines to provide a strategy to overcome resistance to kinase inhibitor therapy.

INTRODUCTION

Small-molecule inhibitors of kinases of the PI3K pathway (PI3K, AKT, mTOR) have therapeutic value in cancers that contain lesions in the PI3K pathway; however, many of the tumors with mutations in the pathway are resistant to treatment (Bendell et al., 2012; Elkabets et al., 2013; Janku et al., 2012; She et al., 2008). Resistance to therapy has in some instances been traced to short-lived inhibition of the pathway that is due to feedback activation of the transcription of tyrosine kinase genes in the insulin receptor, and EGFR and JAK families (Britschgi et al., 2012; Chandarlapaty et al., 2011; O'Reilly et al., 2006; Rodrik-Outmezguine et al., 2011; Serra et al., 2011). Inhibitors of receptor tyrosine kinases (RTKs) can ameliorate feedback to restore lower PI3K signaling, but this approach has its limitations since the repertoire of receptors activated by feedback in any given tumor is unpredictable. Resistance to PI3K inhibitors can also be demonstrated through amplification of *MYC* and *EIF4E* and overexpression of RSK kinases, all of which regulate protein translation (Ilic et al., 2011; Liu et al., 2011; Serra et al., 2013).

Members of the BET family of proteins (BRD2, BRD3, BRD4, and BRDT) contain two tandem bromodomains that recognize acetylated-lysine residues in nucleosomal histones, facilitating the recruitment of transcriptional proteins to chromatin (Filippakopoulos et al., 2010). Small-molecule inhibitors of BETs show a wide range of activity in different types of cancer through their ability to alter the epigenetic landscape by interfering with BRD4, which is required for enhancer function and transcriptional elongation (Delmore et al., 2011; Filippakopoulos et al., 2010; Rahl et al., 2010). Pharmacological inhibition of BET proteins has been shown to lower the expression of a variety of genes that are crucial for cell lineage and viability in several types of malignancy (Asangani et al., 2014; Bandopadhayay et al., 2014; Cho et al., 2014; Dawson et al., 2011; Delmore et al.,

Significance

Activation of feedback loops following inhibition of PI3K/AKT, BRAF, and MEK/ERK can lead to drug resistance and has been associated with upregulation of RTKs. However, the repertoire of receptors activated by feedback in any given tumor is not yet predictable, prompting the need for combination treatments that would be applicable in multiple tumor settings. We have found that combined PI3K and BET inhibition overcomes feedback activation of the PI3K pathway and leads to durable blockage of the PI3K signal in many types of cancer, cell death, and regression of allografted mammary tumors. These findings provide the rationale for combining kinase and epigenetic inhibitors to improve therapy through blocking feedback activation of signaling pathways in several human cancers.

2011; Lockwood et al., 2012; Lovén et al., 2013; Segura et al., 2013; Shi et al., 2014; Whyte et al., 2013; Zuber et al., 2011).

Mitogenic signaling through RTKs activates PI3K to activate AKT and mTOR to enhance MYC mRNA translation, MYC protein half-life, and MYC transcriptional activity (Gera et al., 2004; Yeh et al., 2004; Zhu et al., 2008). Moreover, inhibition of PI3K pathway kinases is able to lower MYC levels in some cellular contexts, and it has been established that activation of this upstream kinase cascade is required for cell transformation by MYC (Lynch et al., 2004). Phosphoinositide-3 kinase (PI3K) and MYC are therefore arguably components of the same signaling pathway that coordinate metabolic signals to increase cell proliferation (Hay and Sonenberg, 2004). Activation of this pathway occurs through mutation of its major nodes, including activating mutations of *PIK3CA*, amplification of *ERBB2*, mutation of *AKT1*, loss of function mutations of *PTEN* (Bader et al., 2005; Manning and Cantley, 2007), and increased genomic copy number, mutation, or chromosomal translocation of *MYC* (Soucek and Evan, 2010). Many of these mutations co-occur within the same tumor, including *PIK3CA* and *MYC* in breast cancer (Liu et al., 2011). Alteration of PI3K and MYC has long been known to cooperate in cellular transformation (Zhao et al., 2003). The therapeutic repercussion for such co-occurrence is high, because amplification of *Myc* in mouse mammary tumors initiated with a *Pik3ca* mutation renders them resistant to PI3K inhibition (Liu et al., 2011). Here, using a metastatic breast cancer model driven by mutations in PI3K and MYC that is resistant to PI3K inhibition, we set out to identify a treatment strategy that overcomes resistance to PI3K inhibition and then determined its effectiveness in multiple tumor types and genetic contexts.

RESULTS

PI3K and MYC Pathways Cooperate in Mouse Mammary Tumorigenesis

While studying the role of *Myc* in mouse mammary tumorigenesis using MMTV-*Myc* transgenic mice (Stewart et al., 1984), we found absence of PTEN staining through immunohistochemistry (IHC) in ~70% of *Myc* tumors, which was accompanied with reduced *Pten* mRNA (Figures 1A–1C and S1A; Table S1). To test the hypothesis that somatic activation of the PI3K pathway is a critical step in the evolution of MMTV-*Myc* tumors we crossed MMTV-*Myc* mice with conditional *Pik3ca* hotspot mutants (H1047R or E545K) (Figures S1B–S1D) or $Pten^{flox/flox}$ mice (Li et al., 2002). Expression of the mutant *Pik3ca* or deletion of *Pten* in alveolar and ductal mammary epithelial cells was driven by Cre that was expressed from the *Wap* locus (Ludwig et al., 2001) and was achieved through mating. Because of the difference in the onset of MMTV and Wap promoter activation, this is a faithful "two-hit" model where deregulated *Myc* expression is effective in virgin females and activation of the PI3K pathway is pregnancy/lactation dependent.

In contrast to *Myc* overexpressing females, which developed focal mammary tumors with a median tumor latency (T_{50}) of 115 days after the first parturition, invasive carcinomas appeared in MMTV-*Myc*;$Pik3ca^{E545K/+}$;Wap^{Cre} (*EK;Myc*), MMTV-*Myc*;$Pik3ca^{H1047R/+}$;Wap^{Cre} (*HR;Myc*), MMTV-*Myc*;$Pten^{flox/+}$;Wap^{Cre} ($Pten^{del/+}$;*Myc*), and MMTV-*Myc*;$Pten^{flox/flox}$;Wap^{Cre} ($Pten^{del/del}$;*Myc*) animals (collectively referred to as *PI3K;Myc*) within approximately 1 week after the first parturition (Figure 1A). A requirement for a second pregnancy was recorded in only 3/21 *EK;Myc,* 1/18 *HR;Myc*, 2/13 $Pten^{del/+}$;*Myc*, and none of the $Pten^{del/del}$;*Myc* females. Mammary tumors, which were palpable in many *PI3K;Myc* animals soon after the delivery of pups, could involve more than one gland and were multifocal. Moreover, they were always associated with widespread mammary intraepithelial neoplasia (Figure S1E).

Comparative histopathological analysis showed that the *PI3K;Myc* tumors had largely retained features characteristic of *Myc*-induced adenocarcinomas (Andrechek et al., 2009; Cardiff et al., 1991), consistent with previous observations indicating that the *Myc* phenotype is dominant in combination with other oncogenes (Cardiff et al., 1991). Thus, all invasive tumors were composed of large cells with amphophilic cytoplasm and giant, highly pleomorphic nuclei containing prominent nucleoli arranged in solid nests with abortive ductal structures (Figure 1C). *PI3K;Myc* tumors were strongly positive for the basal keratins 5 and 14 (CK5 and CK14), showed variable expression of the luminal keratin 18 (CK18), and were negative for ERα and PR (Figure S1F; Table S1). Pulmonary micrometastases, which were strongly positive for CK5, were present in ~85% of *PI3K;Myc* tumors, suggesting that these tumors are competent to metastasize soon after their establishment (Figure S1G). Interestingly, loss of Pten expression in either *Myc*-only or $Pten^{del/+}$;*Myc* and $Pten^{del/del}$;*Myc* tumors was associated with a predominantly membranous p-AKT (S473) immunostaining, which was not seen in *EK;Myc* and *HR;Myc* tumors (Figures 1B and 1C; Table S1).

PI3K;Myc Tumor Cells Are Resistant to PI3K or BET Inhibition

The extreme rapidity of *PI3K;Myc* tumor onset indicates that activation of PI3K and MYC is sufficient to drive mammary tumorigenesis in mice and suggested that inhibition of these oncogenes might be an effective way to treat these tumors. To dissect dependence on PI3K and MYC and identify potential mechanisms of intrinsic resistance to targeted therapy, we used fresh tumor specimens to generate *HR;Myc* (MCCL-278) and $Pten^{del/del}$;*Myc* (MCCL-357) cancer lines. These cell lines were validated for elevated expression of MYC and expression of the H1047R *Pik3ca* mutation or loss of PTEN expression, respectively, and both were capable of growing mammary tumors when injected into the mammary fat pad of immunocompromised mice (Figure 2A). Allografted tumors grew with extreme rapidity, retained the same histological features, showed the same pattern of p-AKT immunostaining, and were highly metastatic to the lungs of the recipient animals (Figure 2B), suggesting that they shared the key features of the primary tumors.

Recent work has established that effective inhibition of the PI3K signal in tumors requires inactivation of both p110α and p110β (Costa et al., 2015; Jia et al., 2008; Schwartz et al., 2015; Torbett et al., 2008; Wee et al., 2008). We therefore treated our mouse cancer cell lines for 5 days with 0.125–8 μM of GDC-0941, a pan-class I PI3K inhibitor (Folkes et al., 2008), and examined the effects on cell growth using an in vitro proliferation assay. MCCL-278 and -357 cells were highly resistant to GDC-0941 and had half maximal growth inhibitory concentration

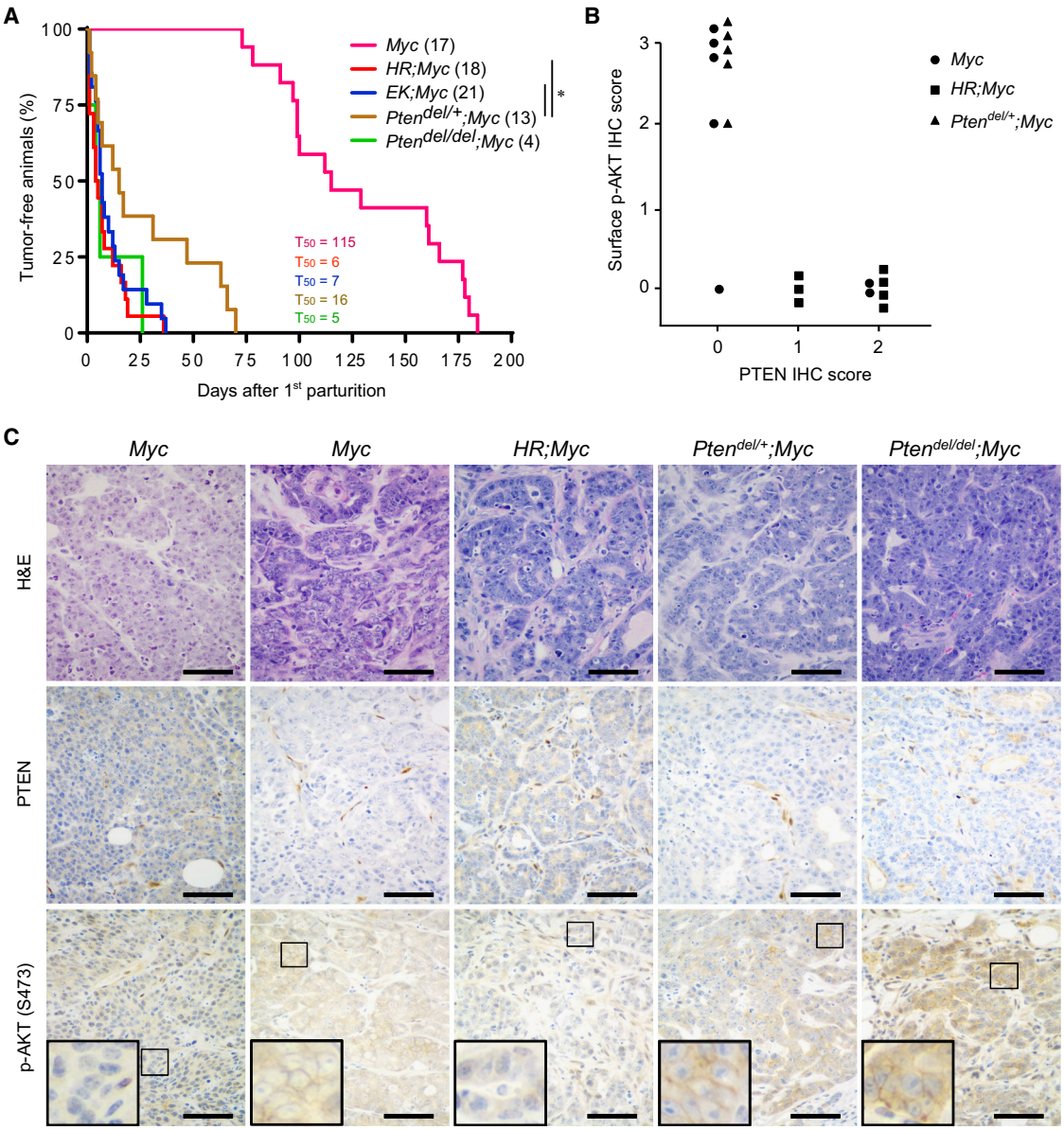

Figure 1. PI3K Pathway Alterations and MYC Cooperate in Mouse Mammary Tumorigenesis

(A) Kaplan-Meier plots of tumor occurrence in cohorts of female mice driven by MMTV-*Myc* and PI3K pathway alterations. The number of mice per cohort is shown in parentheses. T_{50} indicates median tumor latency. *$p < 0.02$.

(B) Scatter plot showing correlation of absence of PTEN and membranous p-AKT (S473) immunostaining in *Pten*$^{del/+}$;*Myc*, *HR;Myc*, and *Myc* mouse tumors. For scoring of immunoreactivity, see Supplemental Experimental Procedures.

(C) Representative sections showing H&E staining and PTEN and p-AKT (S473) immunostaining of mammary tumors in *Myc*, *HR;Myc*, *Pten*$^{del/+}$;*Myc*, and *Pten*$^{del/del}$;*Myc* female mice.

Scale bars, 50 μm. See also Figure S1.

(IC_{50}) values of 2.47 or 4.8 μM, respectively. Residual phosphorylation of AKT was detected at 24 hr, especially at low doses of GDC-0941, and could account for the poor inhibitory effects of cell growth at these doses (Figure 2C). We also detected a dose-dependent downregulation of MYC expression (Figure 2C), likely as a result of reduced translation of *Myc* mRNA and/or increased GSK3β-mediated phosphorylation of MYC on threonine-58 that produces a signal for degradation (Gera et al., 2004; Gregory et al., 2003).

Among the genes that pharmacological inhibition of BET proteins have been recently shown to suppress effectively, *MYC* has been shown in several instances to be important for tumor viability (Asangani et al., 2014; Filippakopoulos et al., 2010; Ilic et al., 2011; Rahl et al., 2010; Segura et al., 2013; Zuber et al., 2011). Because our model is in part driven by MYC, we set out to examine the effects of BET proteins inhibition on cell growth using two different small-molecule inhibitors, JQ1 (Filippakopoulos et al., 2010) and MS417 (Zhang et al., 2012), at the

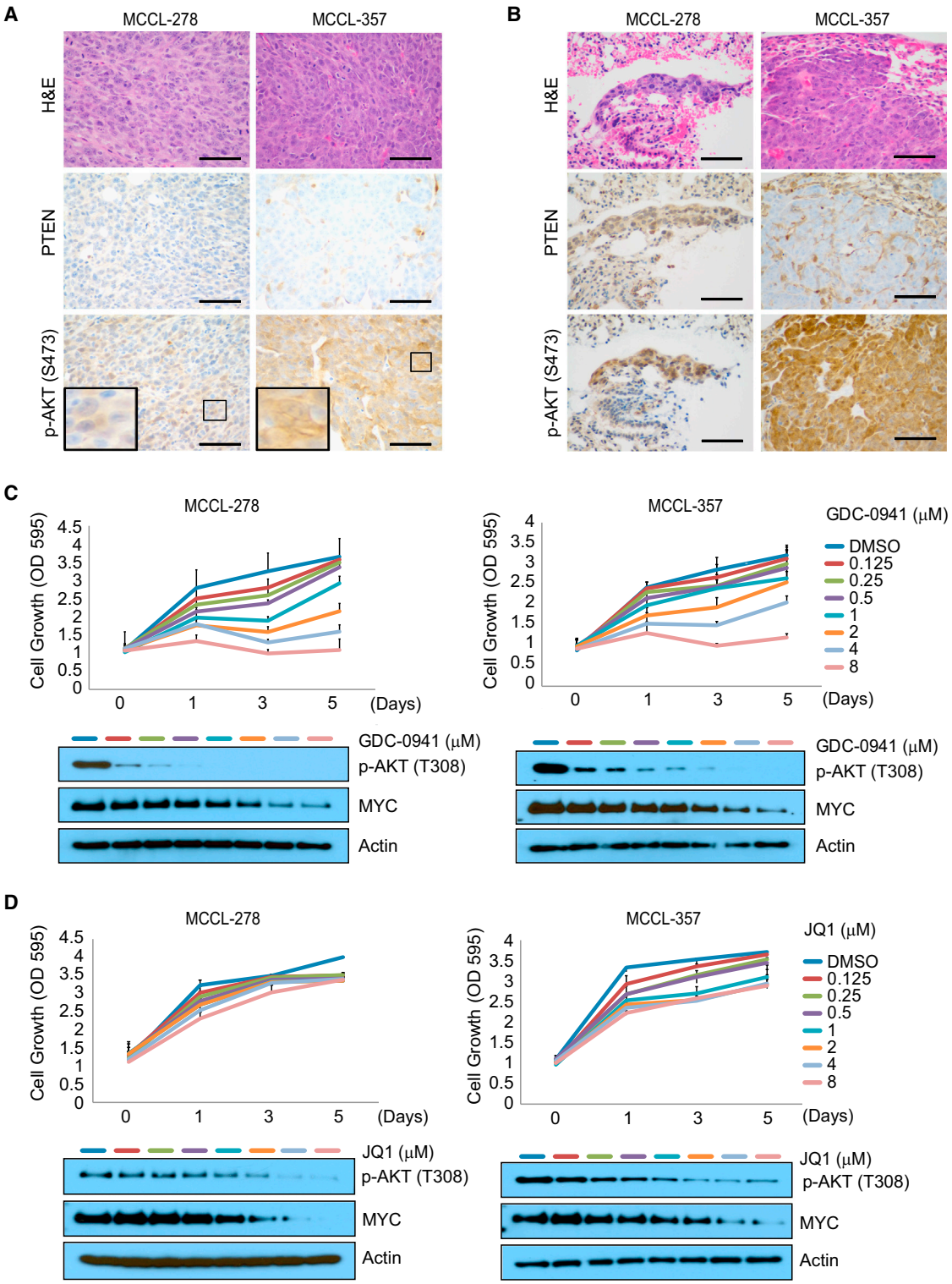

Figure 2. *PI3K;Myc* Cells Are Resistant to PI3K and BET Single Inhibition

(A) Representative sections showing H&E staining and PTEN and p-AKT (S473) immunostaining in mammary tumors from MCCL-278 and -357 allografts. Scale bars, 50 μm.

(B) Representative sections showing H&E staining and PTEN and p-AKT (S473) immunostaining of lung metastases in females with MCCL-278 and MCCL-357 allografted tumors. Scale bars, 50 μm.

(legend continued on next page)

same dose range and time as above. Treatment of MCCL-278 and -357 cells with JQ1 or MS417 failed to inhibit their growth despite lowering MYC protein by 24 hr at high doses ($\geq$4 μM) of the drugs (Figures 2D and S2A). Both BET inhibitors at 1 μM partially lowered *Myc* mRNA at 2 hr to a level that was consistent with what we had observed at the protein level at 24 hr (Figure S2B). Similarly, downregulation of MYC expression using the small hairpin RNA (shRNA) approach failed to block cell growth (Figure S2C). Unexpectedly, BET inhibition lowered AKT phosphorylation in a dose responsive manner, suggesting an unknown role of BET proteins in the activation of AKT (Figure 2D).

We next sought to test the effects of PI3K or BET inhibition in SUM-159 cells, a human breast cancer cell line that is mutant for *PIK3CA*, wild-type for *PTEN*, and has a focal amplification in the *MYC* locus (Fernandez et al., 2013). Similar to the resistant *PI3K;Myc* mouse cells, SUM-159 cells were resistant to either PI3K (GDC-0941 IC_{50} = 2.31 μM) or BET (JQ1 IC_{50} > 8 μM) inhibition, and as was seen with the mouse tumor lines, both inhibitors partially lowered AKT phosphorylation and MYC (Figure S2D). Collectively, these data suggest that tumor cells with high MYC levels and concurrent activation of the PI3K pathway are intrinsically resistant to BET or PI3K inhibition.

BET Inhibition Sensitizes *PI3K;Myc* Cells to GDC-0941 Treatment

To examine whether BET inhibition could increase the efficacy of GDC-0941, we treated resistant cells with a fixed dose of GDC-0941 and increasing doses of JQ1 or MS417. In the presence of 1 μM of GDC-0941, significant attenuation of cell growth was accomplished with as low as 0.125 μM of either of the BET inhibitors (Figures 3A, 3B, and S3A). The same results were seen with 1 μM of JQ1 and $\geq$1 μM of GDC-0941 for both mouse cell lines (Figure S3B). Comparison of cell density after 5 days of treatment with 1 μM of GDC-0941 and increasing doses of JQ1 revealed that at least 1 μM of both drugs was required to have a cytostatic effect (Figure 3C). Indeed, treatment of MCCL-357 and SUM-159 cells with 1 μM of GDC-0941 and MS417 led to increased induction of cell death compared with what was achieved with single drug treatments (Figure 3D).

Combined inhibition of multiple nodes in the PI3K pathway has been shown to overcome resistance to kinase-specific inhibitors (Chandarlapaty et al., 2011; O'Reilly et al., 2006; Rodrik-Outmezguine et al., 2011; Serra et al., 2011). To examine how PI3K/BET inhibition compares with other combinatorial treatments, we treated *PI3K;Myc* mouse cells for 3 days with 1 μM of GDC-0941 and 1 μM of inhibitors against receptors of the EGFR family, AKT, mTOR, dual PI3K/mTOR, or PARP. JQ1 treatment sensitized both cell lines to GDC-0941 more than any other inhibitor (inhibition of growth 88.5%–93.3%) or any other inhibitor combination, underscoring the potency of PI3K/BET combined inhibition (Figure 3E).

BET Inhibition Blocks PI3K Pathway Reactivation after GDC-0941 Treatment

To gain more insight into how combined PI3K/BET inhibition leads to effective growth inhibition, we treated MCCL-278, MCCL-357, and SUM-159 cells with JQ1, GDC-0941, or the combination and harvested cells at multiple time points for up to 32 hr. Treatment with JQ1 led to downregulation of the PI3K pathway over time as measured by phosphorylation of AKT and its downstream target PRAS40 as well as a modest suppression of MYC (Figures 4A and S4A). On the other hand, GDC-0941 treatment inhibited phosphorylation of AKT and its downstream substrates FOXO1/O3, GSK3β, and PRAS40 as well as the mTOR substrate 4E-BP1 within 1 hr of treatment (Figures 4B and S4B). However, maximal inhibition of the signaling was only transient since phosphorylation started to rebound at 4–8 hr, indicating that the PI3K pathway was reactivated. PI3K-dependent inhibition of MYC followed the same pattern after treatment with GDC-0941, with reduced expression occurring only at 1 hr, suggesting that it is modulated by the same feedback loop. Remarkably, addition of a BET inhibitor interfered with the rebound of AKT phosphorylation and consequently attenuated reactivation of the downstream pathway all the way to MYC for up to 32 hr in all three cell lines (Figures 4B and S4B).

Inhibition of PI3K or AKT has been shown to induce the transcription and activation of multiple receptor tyrosine kinases (RTKs) that reactivate the pathway (Chandarlapaty et al., 2011; O'Reilly et al., 2006; Rodrik-Outmezguine et al., 2011; Serra et al., 2011). Expression of several RTK proteins including INSR, IGF1R, HER2, and HER3 was indeed induced after 1–8 hr of GDC-0941 treatment, and this phenomenon was markedly blocked by JQ1 (Figures 4B and S4B). Upregulation of mRNA levels for *IGF1R* and *INSR* was also documented at 2 hr of treatment with GDC-0941. However, JQ1 treatment was able to suppress the transcripts of these receptors and alleviate their GDC-0941-mediated induction (Figure 4C).

To provide further evidence that activation of RTKs of the EGFR and INSR families contributes to the escape from growth inhibition due to treatment with GDC-0941, we used pharmacological inhibitors for EGFR/ERBB2 (Lapatinib) and IGF1R/INSR (OSI-906). Both inhibitors were able to partially rescue reactivation of the PI3K signal and improve inhibition of growth of MCCL-357 and SUM-159 cells after treatment with GDC-0941 (Figures 4D, 4E, and S4C). Triple drug treatment efficiently blocked PI3K signal but failed to inhibit cell growth to the same extent as GDC-0941/MS417 dual treatment, suggesting that additional targets are contributing to the growth inhibitory effects of BET inhibition (Figures 4D, 4E, and S4C).

To examine whether reactivation of the PI3K signal is dependent on MYC, we treated control and MYC-knockdown MCCL-357 cells with 1 μM of JQ1, GDC-0941, or their combination. Partial re-activation of the PI3K pathway after treatment with GDC-0941 for 32 hr and upregulation of INSR and IGF1R, but not of HER2 and HER3, was still documented in these cells

(C) Proliferation analysis for MCCL-278 and MCCL-357 cells treated with the indicated concentrations of GDC-0941. Data represent average ± SD of three replicates. Western blot analysis for p-AKT (T308) and MYC after treatment with the same doses for 24 hr is also shown.
(D) Proliferation analysis for MCCL-278 and MCCL-357 cells treated with the indicated concentrations of JQ1. Data represent average ± SD of three replicates. Western blot analysis for MYC and p-AKT (T308) after treatment with the same doses for 24 hr is also shown.
See also Figure S2.

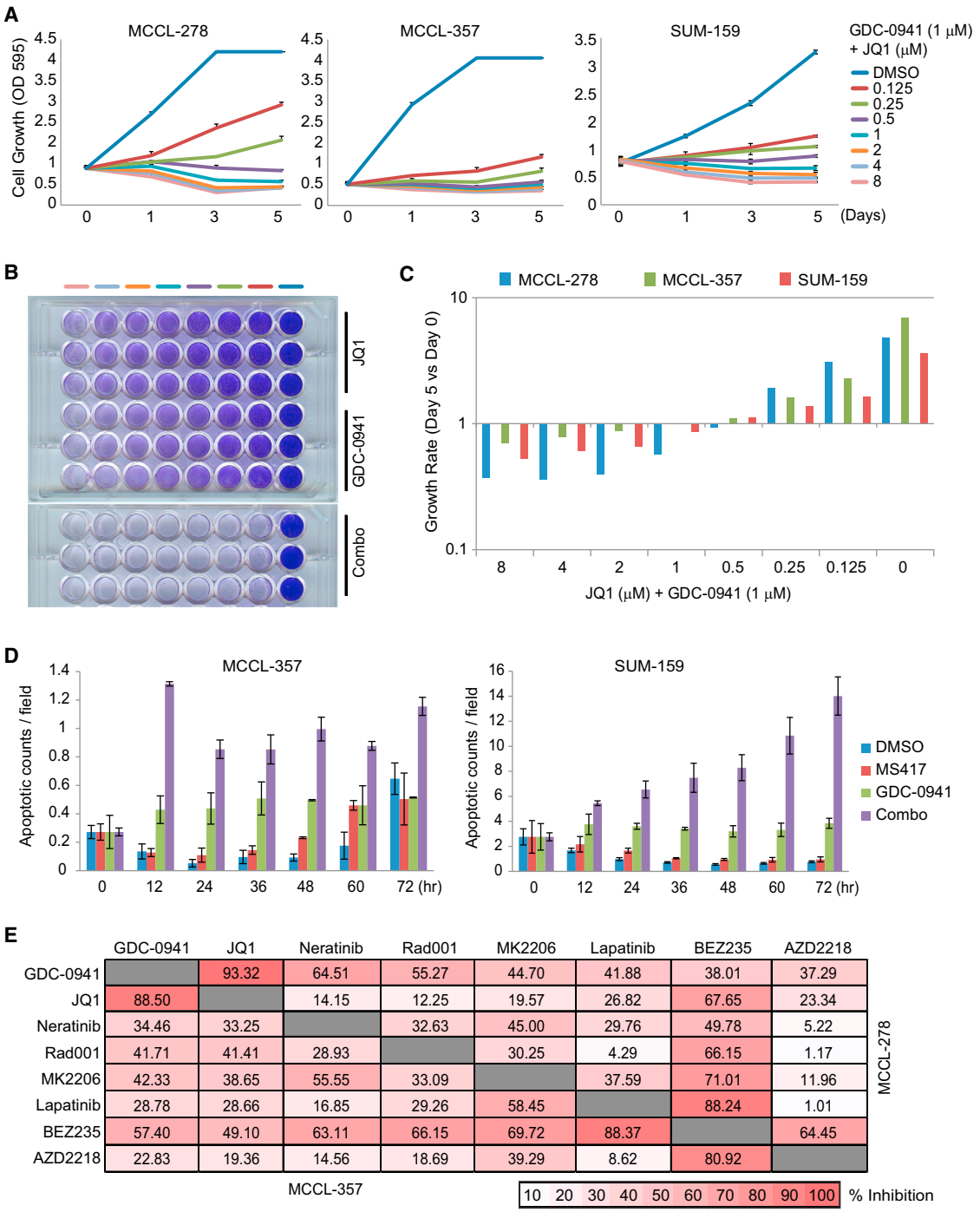

Figure 3. BET Inhibition Sensitizes Resistant Cells to PI3K Inhibition

(A) Proliferation analysis of indicated cells treated with 1 μM of GDC-0941 and the indicated doses of JQ1. Data represent average ± SD of three replicates.

(B) Representative result showing the effects on growth of MCCL-357 cells after treatment with the indicated doses of JQ1, GDC-0941, or the combination at day 5 of treatment.

(C) Fold changes in average cell growth of indicated cells after treatment with 1 μM of GDC-0941 and the indicated doses of JQ1. Values > 1 indicate reduction of total cell numbers.

(D) Indicated cells were treated with 1 μM of GDC-0941, MS417, or their combination for 3 days in the presence of 1.5 μM of DRAQ7. Apoptotic red counts at the indicated time points were calculated using IncuCyte FLR object counting. Data were normalized to confluence and then to DMSO-treated samples and represent average ± SD of three replicates.

(E) Heatmap showing % of inhibition of MCCL-278 and MCCL-357 cell growth after treatment with 1 μM of the indicated inhibitors for 3 days. Data represent average of two replicates.

See also Figure S3.

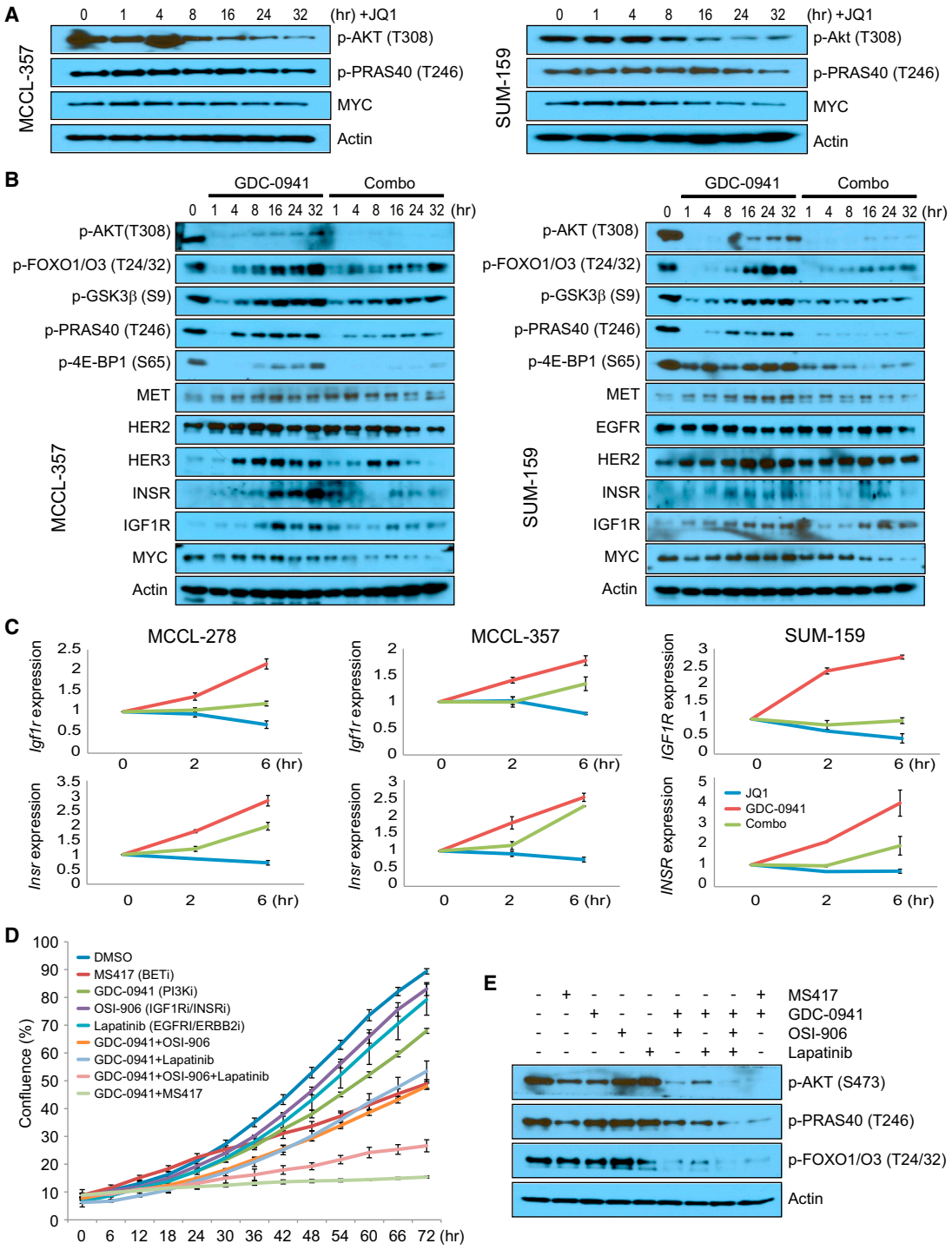

Figure 4. JQ1 Treatment Hinders Feedback Activation of the PI3K Pathway after GDC-0941 Treatment

(A) MCCL-357 and SUM-159 cells were treated with 1 μM of JQ1 for the indicated time points, and the phosphorylation status of AKT and PRAS40 as well as MYC levels were assessed by western blot.

(B) Western blot analysis in MCCL-357 and SUM-159 cells treated with 1 μM of GDC-0941 with or without 1 μM of JQ1 for the indicated time points.

(C) Quantitative RT-PCR for mRNA levels of the indicated receptors in cells treated with 1 μM of GDC-0941 and/or JQ1 relative to DMSO-treated control cells. Results were normalized to actin and error bars indicate ± SD of three independent experiments.

(D) MCCL-357 cells were grown in the presence of 0.5 μM of the indicated inhibitors except for OSI-906, which was dosed at 1 μM, and confluence was calculated for the indicated time points using phase-contrast images. Data represent average ± SD of three replicates.

(E) Western blot analysis in MCCL-357 cells treated with the same doses of the indicated inhibitors as in (D) for 48 hr.

See also Figure S4.

where MYC levels were undetectable (Figure S4D). Together, these data suggest that in MCCL-357 tumor cells BET inhibitors are able to lower PI3K signaling and cooperate with GDC-0941 to inhibit feedback activation of IGF1R and INSR regardless of *MYC*, but feedback activation of HER2 and HER3 requires *MYC*.

Combined PI3K/BET Inhibition Blocks Reactivation of the PI3K Signal in Diverse Cancer Models

To further explore the ability of BET inhibition to block PI3K pathway reactivation after treatment with PI3K inhibitors in human breast cancer, we compared SUM-159 to six additional breast cancer cell lines that harbor mutations in *PIK3CA* or *PTEN* but lack focal amplification of *MYC* (Figure 5A). Treatment with 0.5 μM of GDC-0941 successfully blocked phosphorylation of AKT at 1 hr, but pathway reactivation as measured by phosphorylation of AKT, FOXO1/O3, PRAS40, and/or 4E-BP1 was evident at 24 hr (Figure S5A). Upregulation of specific RTKs was also evident at 24 hr in some of the cell lines, as was MYC (Figures 5A and S5A). Addition of 0.5 μM of MS417 was capable of blocking the GDC-0941-mediated induction of expression of HER3, INSR, and IGF1R in the majority of the cells that were tested (Figures 5A and S5A). Most importantly, the combined PI3K/BET inhibition blocked AKT and mTORC1 reactivation in all seven breast cancer cell lines examined (Figure S5A).

BET inhibitors have been shown to be effective via different targets in a cell lineage-dependent manner (Lovén et al., 2013; Whyte et al., 2013; Asangani et al., 2014; Lockwood et al., 2012; Shi et al., 2014). To examine whether BET inhibition could block PI3K pathway reactivation in other tumor models, we extended our analysis to *PIK3CA*/*PTEN* mutant cells from multiple tumor types (colorectal carcinoma, ovarian carcinoma, prostate carcinoma, and glioblastoma multiforme). Inhibition of PI3K signal after treatment with GDC-0941 was sustained in HCT116 and U-87MG cells but was transient in the rest of the cells with, for example, rebounding of phosphorylation of PRAS40 and/or 4E-BP1 at 24 hr (Figure S5A). Notably, combined BET/PI3K inhibition clamped the PI3K signal and lowered the expression of IGF1R and HER3 in all examined cells that expressed these receptors (Figures 5A and S5A). However, combined treatment lowered the expression of INSR (Figure 5A), EGFR, and HER2 (Figure S5B; data not shown) in some, but not all, cell lines, suggesting that expression of these receptors is not always regulated by BET proteins. As was seen in the human breast cancer lines, upregulation of MYC was often seen after 24 hr of GDC-0941, which was typically rescued by the addition of MS417. Since expression of MYC was either barely detectable in some of the cells (e.g., MCF7, MDA-MB-468, OVCAR-3, U-87MG, and DBTRG-05MG) or was not successfully inhibited by combination treatment in some others (e.g., PC-3, SK-OV-3, IGROV1), we hypothesize that MYC contributes to the regulation of the PI3K signal through BET inhibition in a subset of human tumors (Figure S5A).

Combined treatment resulted in increased inhibition of cell growth compared with what was achieved by single drug treatment in several different cell lines, and this was also accompanied by increased induction of apoptosis (Figures 5B and 5C). Moreover, concurrent treatment with Lapatinib, OSI-906, and GDC-0941 was able to block reactivation of the PI3K signal in BT-549 and RKO-1 cells as a result of treatment with GDC-0941, suggesting that the feedback activation of receptors of the insulin and EGFR families is at least partially responsible for their growth in the presence of the PI3K inhibitor (Figures S5C and S5D). Collectively, these results show that feedback activation of signaling induced by PI3K inhibition can be attenuated by targeting BRD4 and possibly other BET proteins in multiple cancer models and suggest that a co-treatment strategy may be broadly effective in situations where feedback activation limits the efficacy of therapy.

BET Inhibition Dissociates BRD4 from Regulatory Regions of Multiple RTKs

BET inhibitors like JQ1 and MS417 have been shown to display high affinity for both bromodomains in BET family members (BRD2, 3, 4) relative to other bromodomain proteins and prevent binding to acetylated histones and chromatin. To better understand the molecular mechanism underlying the function of BET inhibitors, we analyzed publicly available chromatin immunoprecipitation sequencing (ChIP-seq) data for BRD4 binding at putative regulatory regions of multiple RTKs. Enriched BRD4 occupancy was present at conserved regions upstream the transcriptional start site (TSS) of multiple RTKs (sites A) and *MYC* as well as specific intronic regions (sites B) of *IGF1R* and *INSR* (Figures 6A, 6B, and S6A) in HeLa and HEK293T cells (Liu et al., 2013). Increased BRD4 binding was also present at the same sites in MM.1S cells, a multiple myeloma cell line (Lovén et al., 2013), and this was dramatically reduced after treatment with 0.5 μM of JQ1 for 6 hr (Figures 6A, 6B, and S6A). Interestingly, increased BRD4 binding that was susceptible to treatment with JQ1 was documented exclusively after growth stimulation with serum at putative regulatory regions of *Her3* and *Igf1r* in NIH 3T3 cells (Kanno et al., 2014), suggesting that in certain contexts regulation of expression of some BRD4 targets may be dependent on specific mitogenic stimuli (Figure S6B).

To determine if RTKs are direct targets of BRD4 in our model, we performed ChIP experiments in multiple cell lines using an affinity-purified anti-Brd4 antibody. Primers upstream of the TSS of *IGF1R*, *INSR*, *HER3*, and *MYC* as well as intragenic regions for *IGF1R* and *INSR*, located in regions where enriched BRD4 binding was present in MM.1S cells (sites A and B), were used in ChIP-qPCR to detect the binding of BRD4. Increased BRD4 occupancy compared with IgG control was documented at these sites in BT-549, RKO-1, and PC-3 cells as well as homologous regions in MCCL-357 cells, but no enrichment was present in distinct intronic regions of *IGF1R* and *INSR* (sites C) where BRD4 binding was absent in MM.1S cells (Figures 6C–6E and S6C). Treatment with 0.5 μM of MS417 for 6 hr effectively inhibited BRD4 binding to most of these sites in BT-549, RKO-1, and MCCL-357 cells in the presence or absence of GDC-0941. In the case of PC-3 cells, MS417 was able to suppress induction of BRD4 binding after treatment with 0.5 μM of GDC-0941 (Figure 6D). Inhibition of BRD4 binding after treatment with a BET inhibitor correlated with reduced expression of *IGF1R* and *INSR* in RKO-1, PC-3, and MCCL-357 cells (Figures 4C and S6D). Of note, BET inhibition failed to regulate BRD4 binding at the promoter of *MYC* in PC-3 cells (Figure S6E), which is in accordance with what was previously observed with MYC protein in these cells (Figure S5A). These data identify RTKs of the EGFR and insulin receptor families as direct targets of

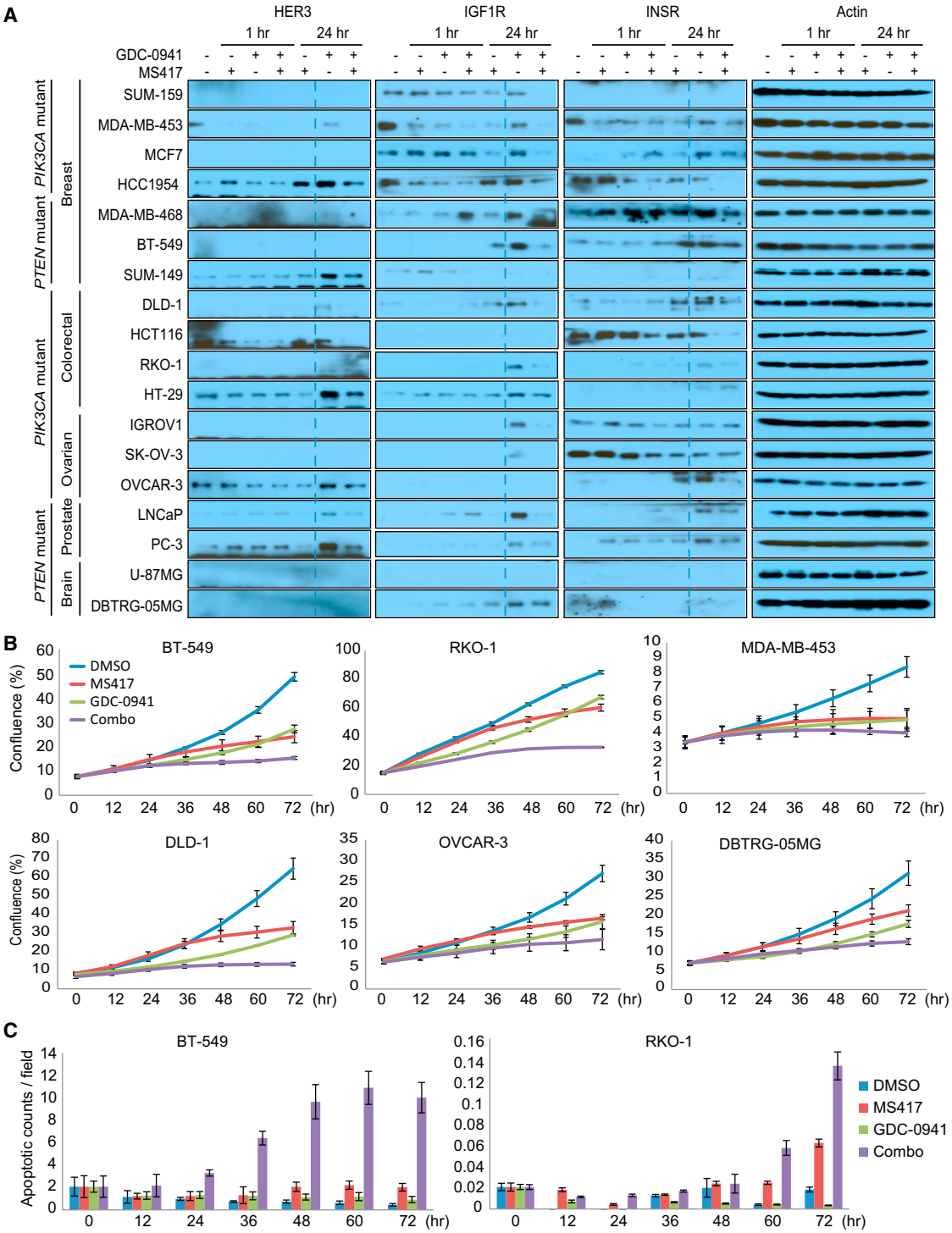

Figure 5. Combined PI3K/BET Inhibition Clamps PI3K Signal and Attenuates Cell Growth in Multiple Tumor Models

(A) Western blot analysis in cells treated with 0.5 μM of GDC-0941 and/or 0.5 μM of MS417 for the indicated time points. Dashed lines were drawn to highlight induction of RTKs after treatment with GDC-0941.

(B and C) Cells were grown in the presence of 0.5 μM of the indicated inhibitors and 1.5 μM of DRAQ7. Confluence (B) was calculated using phase-contrast images and apoptotic counts (C) using IncuCyte FLR object counting. Data represent average ± SD of three replicates.

See also Figure S5.

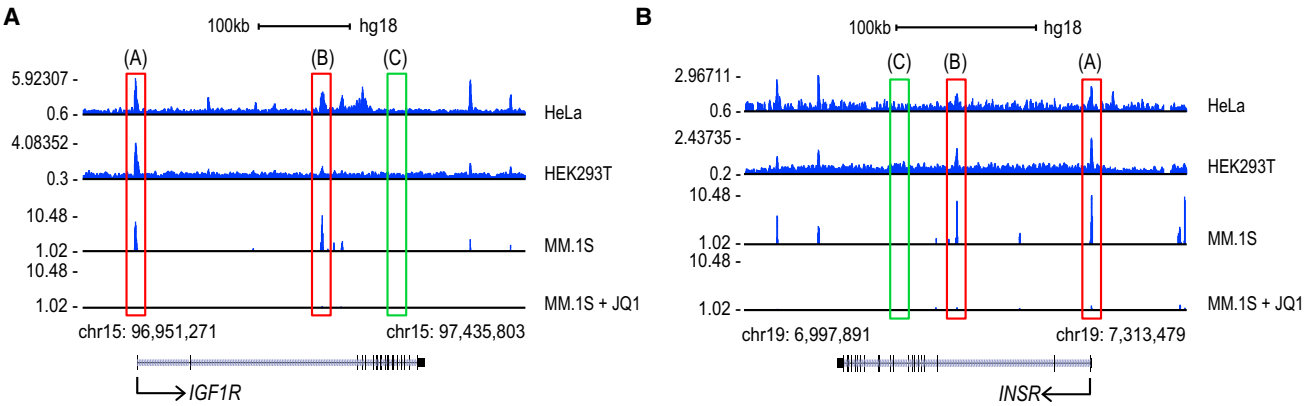

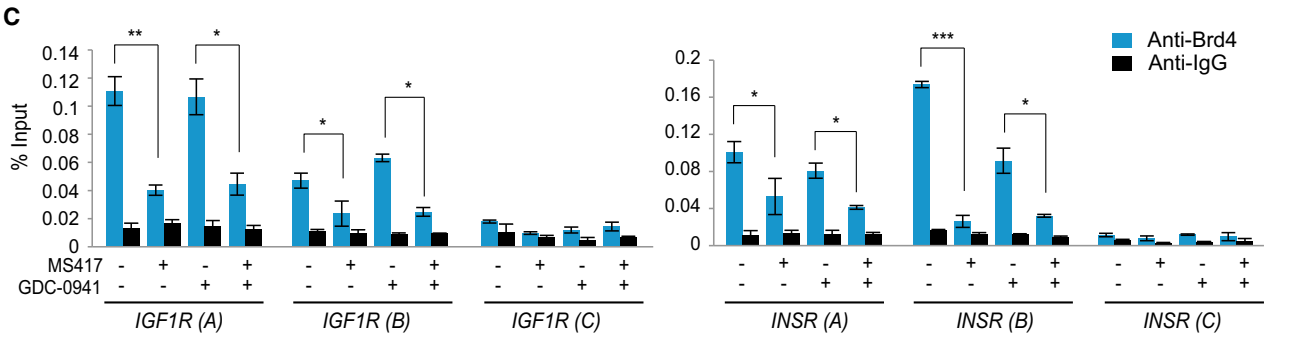

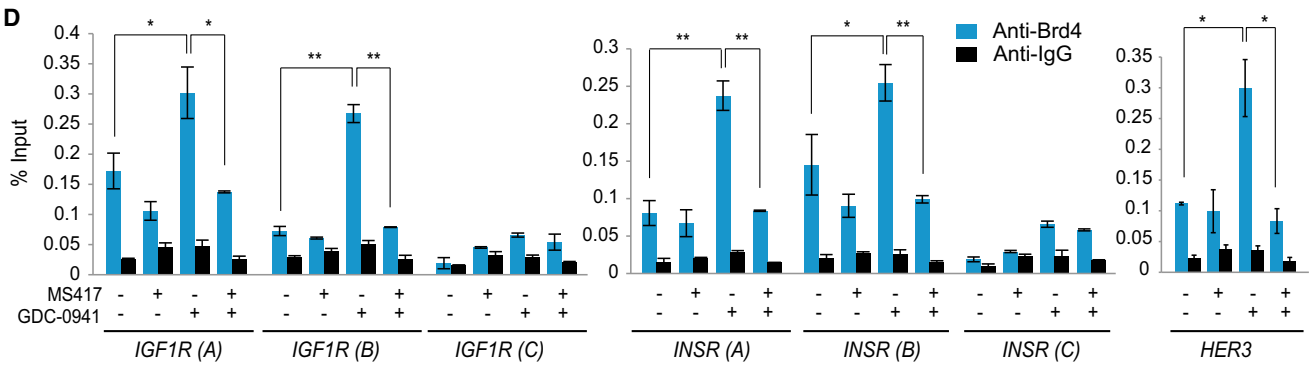

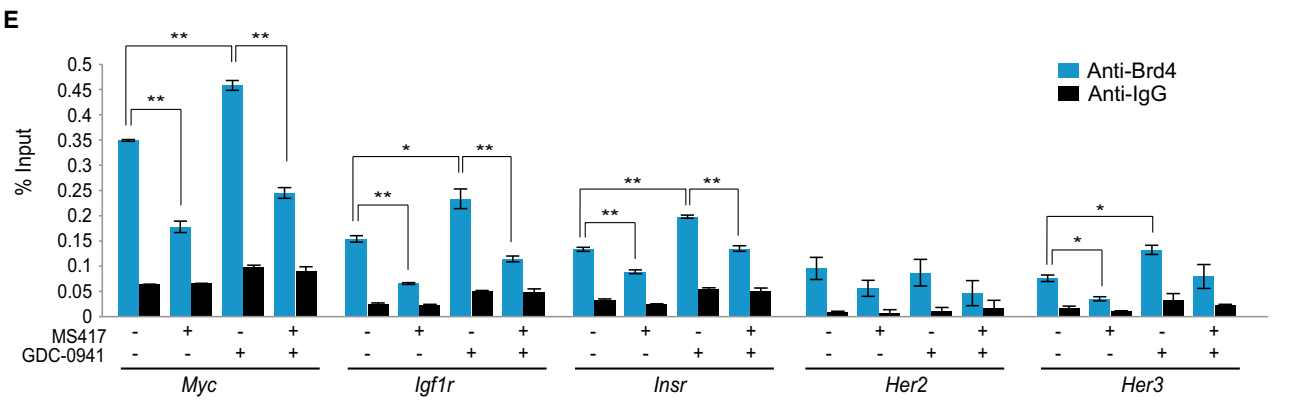

(legend on next page)

BRD4 in several cancer models and strongly suggest that BET inhibition can regulate the PI3K signal in cancer cells by blocking BRD4 recruitment to regulatory regions of these receptors.

Combined PI3K/BET Inhibition Is Effective In Vivo

To test whether PI3K and BET inhibition would inhibit tumor cell growth in vivo, we evaluated the effects of GDC-0941 and/or MS417, which is known to be effective in mice (Shi et al., 2014), in animals engrafted with MCCL-278 and MCCL-357 tumors. Mice were treated with 100 mg/kg/day GDC-0941 and/or 75 mg/kg/day MS417 until tumors in the vehicle-treated animals reached the allowed maximum tumor size. BET inhibition resulted in modest inhibition of tumor growth for both allografted cell lines, and this was accompanied by minimal suppression of MYC and the PI3K signal (Figures 7A–7C). In a similar fashion, treatment with GDC-0941 attenuated the growth of these tumors but only partially inhibited PI3K and mTOR signaling and failed to downregulate MYC. Importantly, mice treated with the combination experienced further suppression of PI3K and mTOR signaling and MYC protein (Figure 7C). The dual treatment was superior to any of the single treatments and resulted in significant tumor shrinkage and tumor cell death as evidenced by increased levels of cleaved caspase-3 (Figures 7A–7C).

DISCUSSION

Here, we use genetic data to demonstrate that sequential activation of MYC and PI3K is sufficient to drive tumorigenesis in mice, and most likely in humans, where they tend to co-occur (Liu et al., 2011). Moreover, we show that *Pten* expression is reduced in the majority of tumors driven by MMTV-*Myc*, underscoring the importance of PI3K pathway activation in the evolution of mouse *Myc* tumors. Generating tumors with specific oncogenes has allowed us to dissect dependence on these oncogenes and identify mechanisms involved in the reduced efficacy of single drug use. Our findings show that PI3K and MYC cooperate as part of a single mitogenic signaling pathway to form cancers. Effective treatment of these tumors in an allograft system required an approach that targets multiple nodes in the pathway to maintain downregulation of the PI3K signal (Figure 7D). One relevant insight of these studies is that it can be inferred that if the PI3K signal is clamped for a sufficient period of time, tumor cell death can occur. The implication for therapy is that combined treatment for several days to achieve maximal tumor cell killing could be sufficient to have a beneficial anti-tumor effect and would not have to be continuous. Although our findings are promising, further work will be needed in additional models and in human clinical trials to determine the ultimate efficacy of combining PI3K and BET inhibitors and whether there will be a sufficient therapeutic window.

Because of the importance of PI3K pathway activation, multiple inhibitors targeting this pathway are currently under development (Martini et al., 2013). However, feedback activation of tyrosine kinase receptors (Britschgi et al., 2012; Chandarlapaty et al., 2011; O'Reilly et al., 2006; Rodrik-Outmezguine et al., 2011; Serra et al., 2011) can account for intrinsic resistance to PI3K inhibition. Alternatively, signals that activate MYC, such as the WNT (Tenbaum et al., 2012), Notch (Muellner et al., 2011), AKT (Zhu et al., 2008) or RSK pathways (Serra et al., 2013; Zhu et al., 2008) as well as MYC itself (Ilic et al., 2011; Liu et al., 2011) or its downstream target eIF4E (Ilic et al., 2011), are all able to confer resistance to PI3K inhibitors. Combining PI3K inhibitors with inhibitors against specific RTKs has been shown to be efficacious in specific models but may have limited utility because of difficulty in predicting the repertoire of receptors that are activated by feedback and the problem of PI3K-independent activation of MYC by amplification or other means. On the basis of our results, a BET inhibitor could be more effective than a tyrosine kinase-specific inhibitor at clamping PI3K reactivation by blocking the expression of multiple RTKs and potentially other unknown factors that would otherwise lead to reactivation of the PI3K pathway caused by GDC-0941. This could involve INSR, IGF1R, EGFR, HER2, and HER3, which were successfully inhibited by MS417 in some of the studied cell lines, and receptors of the PDGF family that can also activate the PI3K pathway. Finally, BET inhibitors have the advantage of being able to reduce MYC function as a transcription and transcription-elongation factor (Delmore et al., 2011; Rahl et al., 2010), which could possibly overcome resistance due to MYC, which we have shown can contribute to feedback activation of HER2 and HER3 expression in some instances.

BET inhibitors affect the expression of a wide range of cancer-relevant targets including MYC, estrogen receptor (Feng et al., 2014), and multiple classes of kinases and other signaling proteins. Because of their broad efficacy, they may be clinically useful in other settings where activation of feedback loops plays a role in intrinsic or acquired resistance to targeted therapy. For instance, ERBB2+ breast cancer cells with acquired resistance to an ERBB2/EGFR inhibitor through the activation of expression of diverse kinases have their sensitivity restored with a BET inhibitor, which was able to target kinases (ERBB3/FAK/EPH/DDR1) contributing to resistance (Stuhlmiller et al., 2015). RAF inhibitors can only transiently inhibit the ERK pathway as they de-repress transcription of *HER3* in thyroid tumor cells (Montero-Conde et al., 2013) and *EGFR* in BRAF (V600E) mutant colon tumor cells (Prahallad et al., 2012). Activation of RTKs has been documented after MEK inhibition in breast tumor cells resulting in ERK pathway reactivation (Duncan et al., 2012). Therefore, it is possible that combined kinase and epigenetic targeting in cancer can be a general strategy to circumvent feedback-mediated resistance from inhibition of other kinases besides PI3K.

In combination with PI3K inhibition, BET inhibition was able to block all or some portion of PI3K signal reactivation in all the

Figure 6. BET Inhibition Blocks BRD4 Binding at Regulatory Regions of RTKs in Multiple Tumor Models

(A and B) Tracks show BRD4 binding across the *IGF1R* (A) and *INSR* (B) loci in the indicated cells with or without treatment with 0.5 μM of JQ1 for 6 hr. Sites A, B, and C indicate the regions where primers were designed to test for the binding of BRD4 in ChIP-qPCR experiments.

(C–E) ChIP-qPCR analysis of BRD4 binding at the indicated sites in RKO-1 (C), PC-3 (D), and MCCL-357 (E) cells treated with 0.5 μM of GDC-0941, MS417, or their combination for 6 hr. Data represent average ± SD of two qPCR experiments. *$p < 0.05$, **$p < 0.01$, ***$p < 0.001$.

See also Figure S6.

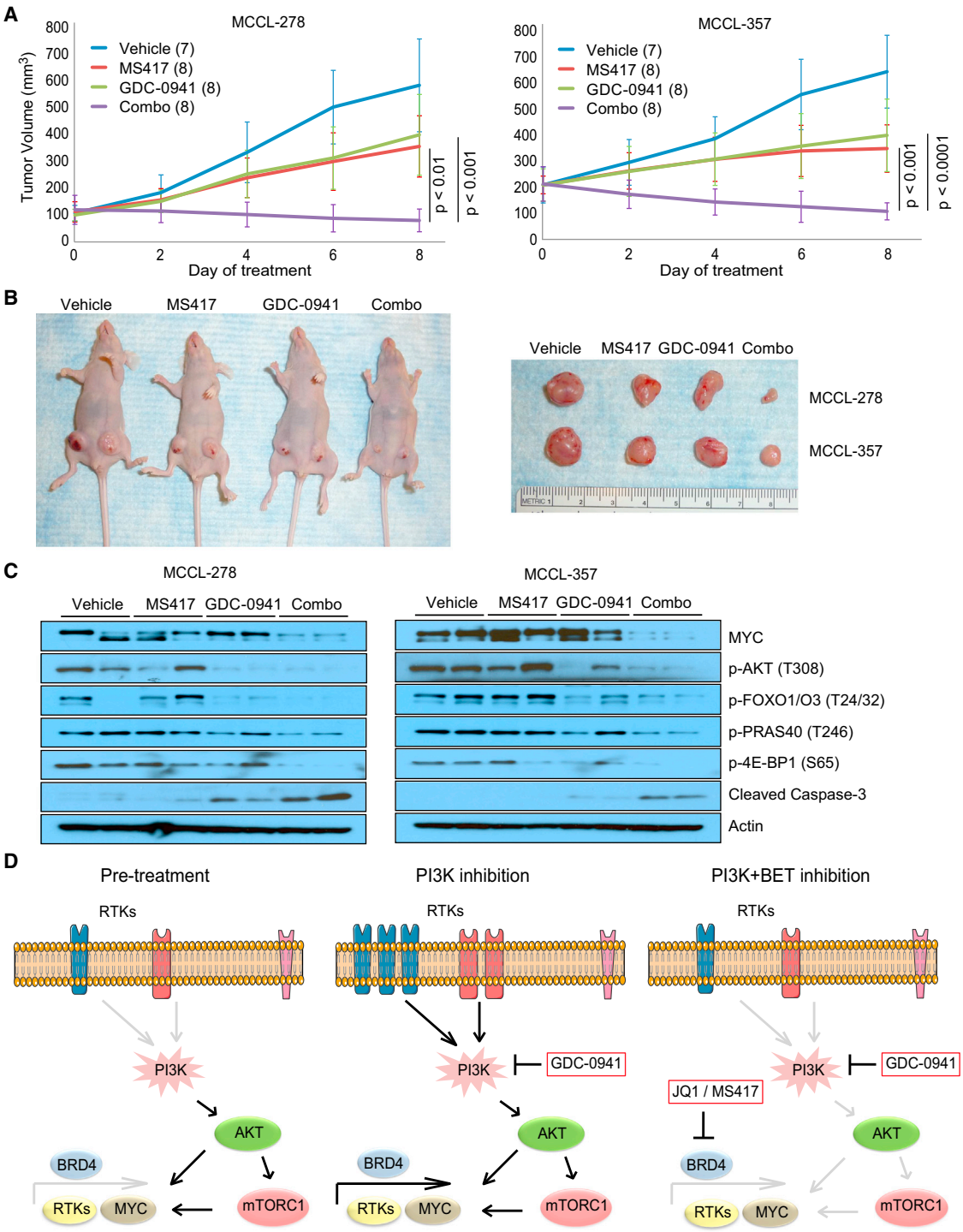

Figure 7. Antitumor Efficiency of PI3K and BET Inhibition In Vivo

(A) MCCL-278 and MCCL-357 allografts were treated with GDC-0941, MS417, or their combination. Number of mice per arm is shown in parentheses, and error bars indicate ± SD. The p values were calculated using Sidak's multiple comparisons test.

(B) Representative tumors from mice (MCCL-278 left flank and MCCL-357 right flank) treated with the indicated drugs.

(C) MCCL-278 and MCCL-357 allografts were treated for 72 hr with the indicated drugs, at which point tumors were harvested and snap frozen. Effects of treatments on MYC, markers of the PI3K pathway, and induction of cleavage of Caspase-3 as an indicator of apoptosis were assessed by western blot. Results from two different animals per treatment group are shown here.

(D) A schematic representation of signaling responses to inhibition of PI3K and PI3K/BET combination.

human and mouse tumor cells that were examined. The combined use of BET and PI3K inhibitors may be useful in a setting in which MYC is or is not a driver oncogene because of the ability of BET inhibitors to broadly inhibit feedback activation of the PI3K pathway after treatment with a PI3K inhibitor through its interaction with receptor gene chromatin. Our examination of 20 lines showed that the combination led to a sustained inhibition of the PI3K and mTOR signals and tumor cell death in many of the lines tested. Indeed, basal levels of MYC protein were very low in several of the cells that were studied or BET inhibition failed to inhibit BRD4 binding at the promoter of MYC or suppress its expression in some cell lines (e.g., PC-3), suggesting that MYC itself was not required for the ability of BET inhibitors to regulate RTK expression. Our findings reveal that regulation of PI3K through BETs is a cancer cell protective feedback mechanism that can be exploited for therapy in a variety of tumor types when feedback contributes to therapeutic resistance. Further studies are necessary to determine the therapeutic benefit of combining these inhibitors in a clinical setting.

EXPERIMENTAL PROCEDURES

Generation of *Pik3ca*$^{E545K/+}$ and *Pik3ca*$^{H1047R/+}$ Mice

To generate *Pik3ca*$^{E545K/+}$ and *Pik3ca*$^{H1047R/+}$ mice, we used site-directed mutagenesis to introduce point mutations in codons 545 of exon 9 (E545K) and 1047 of exon 20 (H1047R) and a DNA sequence in the upstream intronic regions consisting of the following components: *loxP* site, splice acceptor site, neomycin-resistance gene driven by the *Pgk* gene promoter, transcriptional "stop" sequence (triple SV40 polyadenylation signal), and *loxP* site. Both models were validated for proper expression of the mutated proteins (see Supplemental Experimental Procedures and Figure S1). Experiments involving mice were performed according to Columbia University and Mount Sinai School of Medicine Institutional Animal Care and Use Committee approved protocols.

Proliferation and Apoptosis Assays

Experiments were carried out in 48-well plates in triplicates. 5–10 × 10^3 cells per well were grown in the presence of various doses of JQ1, MS417, and/or GDC-0941 for 5 days and were treated with fresh drugs at day 3. At the indicated time intervals, cells were washed once with PBS, stained with 0.05% crystal violet in formalin at room temperature for 20–30 min, and washed again twice with PBS before extracting the dye with 10% acetic acid. Plates were then shaken on a microplate shaker at medium speed for at least 1 hr, and the absorbance, corresponding to cell numbers attached on the plates, was measured at 595 nm on a multi-well plate reader (Bio-Rad). Alternatively, 1–3 × 10^3 cells were seeded in 96-well plates in triplicates and drugged at the indicated doses in the presence of 1.5 μM DRAQ7 (Cell Signaling #7406). Cells were then monitored using the IncuCyte live cell imaging system (Essen BioScience), which was placed in a cell culture incubator operated at 37°C and 5% CO_2. Cell confluence was determined using calculations derived from phase-contrast images. Apoptotic red counts were measured in an IncuCyte FLR automated incubator microscope.

Establishment of Mouse Mammary Cancer Cell Lines

Tumor tissue was finely minced and cell aggregates were trypsinized for 10–15 min. Trypsin was inactivated using regular mouse embryonic fibroblasts (MEF) medium, and single cells were generated with mechanical pipetting. Both MCCL-278 and MCCL-357 cell lines were cultured thereafter using regular MEF medium and were routinely passaged twice a week. Cells were tested negative for all tests of the Infectious Microbe PCR Amplification Test (IMPACT).

Cell Infections

For Myc downregulation experiments, MISSION Lentiviral Transduction Particles were purchased from Sigma-Aldrich (clone IDs: TRCN0000-042514, -042515, -234924, -234925, -234926) and used according to the manufacturer's instructions. Briefly, ~10^5 cells were transduced with the viral particles at a MOI = 20 along with a final concentration of 8 μg/mL polybrene. Cells were selected with puromycin at 1 μg/ml for 10 days and then used immediately for signaling and cell growth analysis.

In Vivo Treatment Studies

Approximately 6- to 8-week-old female nude mice (Taconic) were injected subcutaneously with 0.5 × 10^6 MCCL-278 and 1 × 10^6 MCCL-357 cells in MEF media in the left and right flank, respectively. Females bearing tumor grafts were randomized in groups of seven to eight mice per group when tumor volumes reached ~100 mm^3 (MCCL-278) and ~200 mm^3 (MCCL-357). Animals were treated by oral gavage with GDC-0941 at 100 mg/kg/d (dissolved in 10% DMSO, 5% Tween 20, 85% water) and/or by intraperitoneal injection with MS417 at 75 mg/kg/d (dissolved in 10% HP-β-CD) for 8 days. Pharmacodynamic measurements were performed after 72 hr of treatment. Tumor volume was calculated as follows: tumor size (mm^3) = (longer measurement × shorter measurement^2) × 0.5. Tumor sizes were recorded every other day over the course of the studies.

SUPPLEMENTAL INFORMATION

Supplemental Information includes Supplemental Experimental Procedures, six figures, and one table and can be found with this article online at http://dx.doi.org/10.1016/j.ccell.2015.05.006.

AUTHOR CONTRIBUTIONS

E.E.S. and R.P. designed the experiments. M.D. preformed cell proliferation assays in mouse cells. A.J.K. performed signaling and cell growth analysis in some human tumor cell lines. M.S. preformed the pathological and IHC analysis. E.E.S. performed the rest of the experiments. C.L. helped with the interpretation of the data. M.-M.Z. donated the MS417 compound. E.E.S. and R.P. wrote the manuscript with input from all authors.

ACKNOWLEDGMENTS

We thank Argiris Efstratiadis for contributing to the generation of Pik3ca knock-in mice and helpful discussions, James E. Bradner for providing JQ1, Poulikos Poulikakos for providing the colorectal cell lines, members of the R.P. laboratory for technical assistance and critical reading of the manuscript, John Seregos for technical assistance, Monica Mendelsohn for help in generating the *Pik3ca* knock-in mice, and Xi Sun for technical assistance. This work was supported by NCI R01 CA129432 and the Stand Up To Cancer (SU2C) PI3K Dream Team, which also provided the other inhibitors used in this study. Additional support was given to R.P. from the Komen Foundation and to E.E.S. from the Department of Defense Breast Cancer Research Program Era of Hope Award BC087596.

Received: September 23, 2014
Revised: April 14, 2015
Accepted: May 7, 2015
Published: June 8, 2015

REFERENCES

Andrechek, E.R., Cardiff, R.D., Chang, J.T., Gatza, M.L., Acharya, C.R., Potti, A., and Nevins, J.R. (2009). Genetic heterogeneity of Myc-induced mammary tumors reflecting diverse phenotypes including metastatic potential. Proc. Natl. Acad. Sci. USA *106*, 16387–16392.

Asangani, I.A., Dommeti, V.L., Wang, X., Malik, R., Cieslik, M., Yang, R., Escara-Wilke, J., Wilder-Romans, K., Dhanireddy, S., Engelke, C., et al. (2014). Therapeutic targeting of BET bromodomain proteins in castration-resistant prostate cancer. Nature *510*, 278–282.

Bader, A.G., Kang, S., Zhao, L., and Vogt, P.K. (2005). Oncogenic PI3K deregulates transcription and translation. Nat. Rev. Cancer *5*, 921–929.

Bandopadhayay, P., Bergthold, G., Nguyen, B., Schubert, S., Gholamin, S., Tang, Y., Bolin, S., Schumacher, S.E., Zeid, R., Masoud, S., et al. (2014).

BET bromodomain inhibition of MYC-amplified medulloblastoma. Clin. Cancer Res. *20*, 912–925.

Bendell, J.C., Rodon, J., Burris, H.A., de Jonge, M., Verweij, J., Birle, D., Demanse, D., De Buck, S.S., Ru, Q.C., Peters, M., et al. (2012). Phase I, dose-escalation study of BKM120, an oral pan-Class I PI3K inhibitor, in patients with advanced solid tumors. J. Clin. Oncol. *30*, 282–290.

Britschgi, A., Andraos, R., Brinkhaus, H., Klebba, I., Romanet, V., Müller, U., Murakami, M., Radimerski, T., and Bentires-Alj, M. (2012). JAK2/STAT5 inhibition circumvents resistance to PI3K/mTOR blockade: a rationale for cotargeting these pathways in metastatic breast cancer. Cancer Cell *22*, 796–811.

Cardiff, R.D., Sinn, E., Muller, W., and Leder, P. (1991). Transgenic oncogene mice. Tumor phenotype predicts genotype. Am. J. Pathol. *139*, 495–501.

Chandarlapaty, S., Sawai, A., Scaltriti, M., Rodrik-Outmezguine, V., Grbovic-Huezo, O., Serra, V., Majumder, P.K., Baselga, J., and Rosen, N. (2011). AKT inhibition relieves feedback suppression of receptor tyrosine kinase expression and activity. Cancer Cell *19*, 58–71.

Cho, H., Herzka, T., Zheng, W., Qi, J., Wilkinson, J.E., Bradner, J.E., Robinson, B.D., Castillo-Martin, M., Cordon-Cardo, C., and Trotman, L.C. (2014). RapidCaP, a novel GEM model for metastatic prostate cancer analysis and therapy, reveals myc as a driver of Pten-mutant metastasis. Cancer Discov. *4*, 318–333.

Costa, C., Ebi, H., Martini, M., Beausoleil, S.A., Faber, A.C., Jakubik, C.T., Huang, A., Wang, Y., Nishtala, M., Hall, B., et al. (2015). Measurement of PIP3 levels reveals an unexpected role for p110β in early adaptive responses to p110α-specific inhibitors in luminal breast cancer. Cancer Cell *27*, 97–108.

Dawson, M.A., Prinjha, R.K., Dittmann, A., Giotopoulos, G., Bantscheff, M., Chan, W.I., Robson, S.C., Chung, C.W., Hopf, C., Savitski, M.M., et al. (2011). Inhibition of BET recruitment to chromatin as an effective treatment for MLL-fusion leukaemia. Nature *478*, 529–533.

Delmore, J.E., Issa, G.C., Lemieux, M.E., Rahl, P.B., Shi, J., Jacobs, H.M., Kastritis, E., Gilpatrick, T., Paranal, R.M., Qi, J., et al. (2011). BET bromodomain inhibition as a therapeutic strategy to target c-Myc. Cell *146*, 904–917.

Duncan, J.S., Whittle, M.C., Nakamura, K., Abell, A.N., Midland, A.A., Zawistowski, J.S., Johnson, N.L., Granger, D.A., Jordan, N.V., Darr, D.B., et al. (2012). Dynamic reprogramming of the kinome in response to targeted MEK inhibition in triple-negative breast cancer. Cell *149*, 307–321.

Elkabets, M., Vora, S., Juric, D., Morse, N., Mino-Kenudson, M., Muranen, T., Tao, J., Campos, A.B., Rodon, J., Ibrahim, Y.H., et al. (2013). mTORC1 inhibition is required for sensitivity to PI3K p110alpha inhibitors in PIK3CA-mutant breast cancer. Sci. Transl. Med. *5*, 196ra199.

Feng, Q., Zhang, Z., Shea, M.J., Creighton, C.J., Coarfa, C., Hilsenbeck, S.G., Lanz, R., He, B., Wang, L., Fu, X., et al. (2014). An epigenomic approach to therapy for tamoxifen-resistant breast cancer. Cell Res. *24*, 809–819.

Fernandez, S.V., Robertson, F.M., Pei, J., Aburto-Chumpitaz, L., Mu, Z., Chu, K., Alpaugh, R.K., Huang, Y., Cao, Y., Ye, Z., et al. (2013). Inflammatory breast cancer (IBC): clues for targeted therapies. Breast Cancer Res. Treat. *140*, 23–33.

Filippakopoulos, P., Qi, J., Picaud, S., Shen, Y., Smith, W.B., Fedorov, O., Morse, E.M., Keates, T., Hickman, T.T., Felletar, I., et al. (2010). Selective inhibition of BET bromodomains. Nature *468*, 1067–1073.

Folkes, A.J., Ahmadi, K., Alderton, W.K., Alix, S., Baker, S.J., Box, G., Chuckowree, I.S., Clarke, P.A., Depledge, P., Eccles, S.A., et al. (2008). The identification of 2-(1H-indazol-4-yl)-6-(4-methanesulfonyl-piperazin-1-yl-methyl)-4-morpholin-4-yl-thieno[3,2-d]pyrimidine (GDC-0941) as a potent, selective, orally bioavailable inhibitor of class I PI3 kinase for the treatment of cancer. J. Med. Chem. *51*, 5522–5532.

Gera, J.F., Mellinghoff, I.K., Shi, Y., Rettig, M.B., Tran, C., Hsu, J.H., Sawyers, C.L., and Lichtenstein, A.K. (2004). AKT activity determines sensitivity to mammalian target of rapamycin (mTOR) inhibitors by regulating cyclin D1 and c-myc expression. J. Biol. Chem. *279*, 2737–2746.

Gregory, M.A., Qi, Y., and Hann, S.R. (2003). Phosphorylation by glycogen synthase kinase-3 controls c-myc proteolysis and subnuclear localization. J. Biol. Chem. *278*, 51606–51612.

Hay, N., and Sonenberg, N. (2004). Upstream and downstream of mTOR. Genes Dev. *18*, 1926–1945.

Ilic, N., Utermark, T., Widlund, H.R., and Roberts, T.M. (2011). PI3K-targeted therapy can be evaded by gene amplification along the MYC-eukaryotic translation initiation factor 4E (eIF4E) axis. Proc. Natl. Acad. Sci. USA *108*, E699–E708.

Janku, F., Wheler, J.J., Westin, S.N., Moulder, S.L., Naing, A., Tsimberidou, A.M., Fu, S., Falchook, G.S., Hong, D.S., Garrido-Laguna, I., et al. (2012). PI3K/AKT/mTOR inhibitors in patients with breast and gynecologic malignancies harboring PIK3CA mutations. J. Clin. Oncol. *30*, 777–782.

Jia, S., Liu, Z., Zhang, S., Liu, P., Zhang, L., Lee, S.H., Zhang, J., Signoretti, S., Loda, M., Roberts, T.M., and Zhao, J.J. (2008). Essential roles of PI(3)K-p110beta in cell growth, metabolism and tumorigenesis. Nature *454*, 776–779.

Kanno, T., Kanno, Y., LeRoy, G., Campos, E., Sun, H.W., Brooks, S.R., Vahedi, G., Heightman, T.D., Garcia, B.A., Reinberg, D., et al. (2014). BRD4 assists elongation of both coding and enhancer RNAs by interacting with acetylated histones. Nat. Struct. Mol. Biol. *21*, 1047–1057.

Li, G., Robinson, G.W., Lesche, R., Martinez-Diaz, H., Jiang, Z., Rozengurt, N., Wagner, K.U., Wu, D.C., Lane, T.F., Liu, X., et al. (2002). Conditional loss of PTEN leads to precocious development and neoplasia in the mammary gland. Development *129*, 4159–4170.

Liu, P., Cheng, H., Santiago, S., Raeder, M., Zhang, F., Isabella, A., Yang, J., Semaan, D.J., Chen, C., Fox, E.A., et al. (2011). Oncogenic PIK3CA-driven mammary tumors frequently recur via PI3K pathway-dependent and PI3K pathway-independent mechanisms. Nat. Med. *17*, 1116–1120.

Liu, W., Ma, Q., Wong, K., Li, W., Ohgi, K., Zhang, J., Aggarwal, A.K., and Rosenfeld, M.G. (2013). Brd4 and JMJD6-associated anti-pause enhancers in regulation of transcriptional pause release. Cell *155*, 1581–1595.

Lockwood, W.W., Zejnullahu, K., Bradner, J.E., and Varmus, H. (2012). Sensitivity of human lung adenocarcinoma cell lines to targeted inhibition of BET epigenetic signaling proteins. Proc. Natl. Acad. Sci. USA *109*, 19408–19413.

Lovén, J., Hoke, H.A., Lin, C.Y., Lau, A., Orlando, D.A., Vakoc, C.R., Bradner, J.E., Lee, T.I., and Young, R.A. (2013). Selective inhibition of tumor oncogenes by disruption of super-enhancers. Cell *153*, 320–334.

Ludwig, T., Fisher, P., Murty, V., and Efstratiadis, A. (2001). Development of mammary adenocarcinomas by tissue-specific knockout of Brca2 in mice. Oncogene *20*, 3937–3948.

Lynch, M., Fitzgerald, C., Johnston, K.A., Wang, S., and Schmidt, E.V. (2004). Activated eIF4E-binding protein slows G1 progression and blocks transformation by c-myc without inhibiting cell growth. J. Biol. Chem. *279*, 3327–3339.

Manning, B.D., and Cantley, L.C. (2007). AKT/PKB signaling: navigating downstream. Cell *129*, 1261–1274.

Martini, M., Ciraolo, E., Gulluni, F., and Hirsch, E. (2013). Targeting PI3K in cancer: any good news? Front Oncol *3*, 108.

Montero-Conde, C., Ruiz-Llorente, S., Dominguez, J.M., Knauf, J.A., Viale, A., Sherman, E.J., Ryder, M., Ghossein, R.A., Rosen, N., and Fagin, J.A. (2013). Relief of feedback inhibition of HER3 transcription by RAF and MEK inhibitors attenuates their antitumor effects in BRAF-mutant thyroid carcinomas. Cancer Discov. *3*, 520–533.

Muellner, M.K., Uras, I.Z., Gapp, B.V., Kerzendorfer, C., Smida, M., Lechtermann, H., Craig-Mueller, N., Colinge, J., Duernberger, G., and Nijman, S.M. (2011). A chemical-genetic screen reveals a mechanism of resistance to PI3K inhibitors in cancer. Nat. Chem. Biol. *7*, 787–793.

O'Reilly, K.E., Rojo, F., She, Q.B., Solit, D., Mills, G.B., Smith, D., Lane, H., Hofmann, F., Hicklin, D.J., Ludwig, D.L., et al. (2006). mTOR inhibition induces upstream receptor tyrosine kinase signaling and activates Akt. Cancer Res. *66*, 1500–1508.

Prahallad, A., Sun, C., Huang, S., Di Nicolantonio, F., Salazar, R., Zecchin, D., Beijersbergen, R.L., Bardelli, A., and Bernards, R. (2012). Unresponsiveness of colon cancer to BRAF(V600E) inhibition through feedback activation of EGFR. Nature *483*, 100–103.

Rahl, P.B., Lin, C.Y., Seila, A.C., Flynn, R.A., McCuine, S., Burge, C.B., Sharp, P.A., and Young, R.A. (2010). c-Myc regulates transcriptional pause release. Cell *141*, 432–445.

Rodrik-Outmezguine, V.S., Chandarlapaty, S., Pagano, N.C., Poulikakos, P.I., Scaltriti, M., Moskatel, E., Baselga, J., Guichard, S., and Rosen, N. (2011). mTOR kinase inhibition causes feedback-dependent biphasic regulation of AKT signaling. Cancer Discov. *1*, 248–259.

Schwartz, S., Wongvipat, J., Trigwell, C.B., Hancox, U., Carver, B.S., Rodrik-Outmezguine, V., Will, M., Yellen, P., de Stanchina, E., Baselga, J., et al. (2015). Feedback suppression of PI3Kα signaling in PTEN-mutated tumors is relieved by selective inhibition of PI3Kβ. Cancer Cell *27*, 109–122.

Segura, M.F., Fontanals-Cirera, B., Gaziel-Sovran, A., Guijarro, M.V., Hanniford, D., Zhang, G., González-Gomez, P., Morante, M., Jubierre, L., Zhang, W., et al. (2013). BRD4 sustains melanoma proliferation and represents a new target for epigenetic therapy. Cancer Res. *73*, 6264–6276.

Serra, V., Scaltriti, M., Prudkin, L., Eichhorn, P.J., Ibrahim, Y.H., Chandarlapaty, S., Markman, B., Rodriguez, O., Guzman, M., Rodriguez, S., et al. (2011). PI3K inhibition results in enhanced HER signaling and acquired ERK dependency in HER2-overexpressing breast cancer. Oncogene *30*, 2547–2557.

Serra, V., Eichhorn, P.J., García-García, C., Ibrahim, Y.H., Prudkin, L., Sánchez, G., Rodríguez, O., Antón, P., Parra, J.L., Marlow, S., et al. (2013). RSK3/4 mediate resistance to PI3K pathway inhibitors in breast cancer. J. Clin. Invest. *123*, 2551–2563.

She, Q.B., Chandarlapaty, S., Ye, Q., Lobo, J., Haskell, K.M., Leander, K.R., DeFeo-Jones, D., Huber, H.E., and Rosen, N. (2008). Breast tumor cells with PI3K mutation or HER2 amplification are selectively addicted to Akt signaling. PLoS ONE *3*, e3065.

Shi, J., Wang, Y., Zeng, L., Wu, Y., Deng, J., Zhang, Q., Lin, Y., Li, J., Kang, T., Tao, M., et al. (2014). Disrupting the interaction of BRD4 with diacetylated Twist suppresses tumorigenesis in basal-like breast cancer. Cancer Cell *25*, 210–225.

Soucek, L., and Evan, G.I. (2010). The ups and downs of Myc biology. Curr. Opin. Genet. Dev. *20*, 91–95.

Stewart, T.A., Pattengale, P.K., and Leder, P. (1984). Spontaneous mammary adenocarcinomas in transgenic mice that carry and express MTV/myc fusion genes. Cell *38*, 627–637.

Stuhlmiller, T.J., Miller, S.M., Zawistowski, J.S., Nakamura, K., Beltran, A.S., Duncan, J.S., Angus, S.P., Collins, K.A., Granger, D.A., Reuther, R.A., et al. (2015). Inhibition of lapatinib-induced kinome reprogramming in ERBB2-positive breast cancer by targeting BET family bromodomains. Cell Rep. *11*, 390–404.

Tenbaum, S.P., Ordóñez-Morán, P., Puig, I., Chicote, I., Arqués, O., Landolfi, S., Fernández, Y., Herance, J.R., Gispert, J.D., Mendizabal, L., et al. (2012). β-catenin confers resistance to PI3K and AKT inhibitors and subverts FOXO3a to promote metastasis in colon cancer. Nat. Med. *18*, 892–901.

Torbett, N.E., Luna-Moran, A., Knight, Z.A., Houk, A., Moasser, M., Weiss, W., Shokat, K.M., and Stokoe, D. (2008). A chemical screen in diverse breast cancer cell lines reveals genetic enhancers and suppressors of sensitivity to PI3K isoform-selective inhibition. Biochem. J. *415*, 97–110.

Wee, S., Wiederschain, D., Maira, S.M., Loo, A., Miller, C., deBeaumont, R., Stegmeier, F., Yao, Y.M., and Lengauer, C. (2008). PTEN-deficient cancers depend on PIK3CB. Proc. Natl. Acad. Sci. USA *105*, 13057–13062.

Whyte, W.A., Orlando, D.A., Hnisz, D., Abraham, B.J., Lin, C.Y., Kagey, M.H., Rahl, P.B., Lee, T.I., and Young, R.A. (2013). Master transcription factors and mediator establish super-enhancers at key cell identity genes. Cell *153*, 307–319.

Yeh, E., Cunningham, M., Arnold, H., Chasse, D., Monteith, T., Ivaldi, G., Hahn, W.C., Stukenberg, P.T., Shenolikar, S., Uchida, T., et al. (2004). A signalling pathway controlling c-Myc degradation that impacts oncogenic transformation of human cells. Nat. Cell Biol. *6*, 308–318.

Zhang, G., Liu, R., Zhong, Y., Plotnikov, A.N., Zhang, W., Zeng, L., Rusinova, E., Gerona-Nevarro, G., Moshkina, N., Joshua, J., et al. (2012). Down-regulation of NF-κB transcriptional activity in HIV-associated kidney disease by BRD4 inhibition. J. Biol. Chem. *287*, 28840–28851.

Zhao, J.J., Gjoerup, O.V., Subramanian, R.R., Cheng, Y., Chen, W., Roberts, T.M., and Hahn, W.C. (2003). Human mammary epithelial cell transformation through the activation of phosphatidylinositol 3-kinase. Cancer Cell *3*, 483–495.

Zhu, J., Blenis, J., and Yuan, J. (2008). Activation of PI3K/Akt and MAPK pathways regulates Myc-mediated transcription by phosphorylating and promoting the degradation of Mad1. Proc. Natl. Acad. Sci. USA *105*, 6584–6589.

Zuber, J., Shi, J., Wang, E., Rappaport, A.R., Herrmann, H., Sison, E.A., Magoon, D., Qi, J., Blatt, K., Wunderlich, M., et al. (2011). RNAi screen identifies Brd4 as a therapeutic target in acute myeloid leukaemia. Nature *478*, 524–528.